European Radiology (2019) 29:31–39
https://doi.org/10.1007/s00330-018-5568-y

MUSCULOSKELETAL

# Single-source dual-energy computed tomography for the assessment of bone marrow oedema in vertebral compression fractures: a prospective diagnostic accuracy study

Torsten Diekhoff[1] · Nils Engelhard[1] · Michael Fuchs[2] · Matthias Pumberger[2] · Michael Putzier[2] · Jürgen Mews[3] · Marcus Makowski[1] · Bernd Hamm[1] · Kay-Geert A. Hermann[1]

Received: 18 March 2018 / Revised: 16 May 2018 / Accepted: 28 May 2018 / Published online: 15 June 2018


## Abstract

**Objectives** To evaluate the diagnostic accuracy of single-source dual-energy computed tomography (DECT) for the detection of bone marrow oedema (BME) in patients with vertebral compression fractures.

**Methods** Patients over 50 years of age with radiographically suspected vertebral compression fracture of the thoracic or lumbar spine were prospectively enrolled. All patients underwent DECT with sequential acquisition of 80 and 135 kVp datasets on a 320-row detector CT scanner and 1.5-Tesla magnetic resonance imaging (MRI) including T1-weighted and short-tau inversion recovery (STIR) sequences. Virtual non-calcium (VNCa) images were reconstructed using a three-material decomposition algorithm. Vertebrae with height loss in CT were scored for the presence of BME in both MRI and DECT and used to determine signal- and contrast-to-noise ratios (SNR and CNR). Contingency analysis using MRI as standard of reference and Fleiss's kappa were calculated. IRB approval was obtained.

**Results** In total 192 vertebral compression fractures in 70 patients (23 men, 47 women; mean age 70.7 years (SD 9.8)) were included in our analysis. DECT showed a reader-dependent sensitivity of 72% and specificity of 70% for BME. Fleiss's kappa was .40 for DECT and .58 for MRI. T1-weighted images had significantly better SNR and CNR compared to STIR, CT, and VNCa ($p < .0001$); however, there was no difference between STIR and VNCa.

**Conclusions** VNCa images depict BME with adequate sensitivity and specificity and can be acquired on a single-source system. Image quality is adequate but trained readers are needed for image interpretation.

**Key Points**

- *Dual-energy CT in a single-source technique can help to detect bone marrow oedema in patients with vertebral compression fractures.*
- *However, given the inferior inter-rater reliability and limited specificity compared to MRI, experienced readers are needed for image interpretation.*
- *Dual-energy CT of the spine has limited sensitivity for the detection of bone marrow oedema in vertebra with previous surgical intervention.*

**Keywords** Fractures, compression · Tomography, x-ray computed · Oedema · Spine

**Electronic supplementary material** The online version of this article (https://doi.org/10.1007/s00330-018-5568-y) contains supplementary material, which is available to authorized users.

✉ Torsten Diekhoff
torsten.diekhoff@charite.de

[1] Department of Radiology, Charité - Universitätsmedizin Berlin, Campus Mitte, Humboldt-Universität zu Berlin, Freie Universität Berlin, Charitéplatz 1, 10117 Berlin, Germany

[2] Department of Spine Surgery, Center for Musculoskeletal Surgery, Charité - Universitätsmedizin Berlin Campus Mitte, Berlin, Germany

[3] Canon Medical Systems Corporation Europe BV, Zilverstraat 1, 2701 RP Zoetermeer, The Netherlands

**Abbreviations**

| | |
|---|---|
| BME | Bone marrow oedema |
| CNR | Contrast-to-noise ratio |
| DECT | Dual-energy computed tomography |
| IVR | Intervertebral ratio |
| SD | Standard deviation |
| SNR | Signal-to-noise ratio |
| STIR | Short-tau inversion recovery |
| VNCa | Virtual non-calcium reconstruction |

## Introduction

Osteoporotic spinal fractures are of growing economic importance, especially in industrial countries with increasingly older populations [1–4]. Among the different osteoporetic fracture patterns, vertebral compression fractures have the highest prevalence (20% in men and 24% in women over the age of 50 years) [5]. Osteoporotic patients have a higher hospitalisation rate and increased in-hospital healthcare utilisation and mortality compared to non-osteoporotic individuals [4, 6]. Therefore, rapid diagnostic workup of these patients is desirable to initiate swift treatment and to reduce healthcare expenditure.

The diagnostic strategy in patients with suspected vertebral compression fracture includes a radiograph to confirm the loss of vertebral body height. Fracture morphology, along with information on the presence of bone marrow oedema (BME) in fresh fractures and intervertebral disc damage provided by magnetic resonance imaging (MRI) enable a treatment decision to be made (e.g. balloon kyphoplasty) and to estimate the prognosis [7–9]. Computed tomography (CT) might be indicated to assess fracture morphology, vertebral stability criteria, presence of displaced fragments and endplate involvement prior to an intervention [10–13]. As MRI is not immediately available [14], it would be desirable, also with regard to speeding up the diagnostic workup, to obtain the information regarding BME with CT, potentially without the need for an additional MRI examination.

Dual-energy CT (DECT) allows assessment of bone marrow changes using virtual non-calcium imaging (VNCa). The technique uses a three-material decomposition algorithm based on the materials fat, water and calcium to reconstruct virtual images containing fat and water but no calcium. Using these images, an increased water content (BME) can be identified by increased bone marrow density measured in Hounsfield units (HU) [15, 16]. Thus, DECT with VNCa allows demonstration of BME [17] in patients with vertebral compression fractures [18–21]. This technique may speed up the diagnostic procedure in patients with osteoporosis-related vertebral compression fractures and thus allow earlier initiation of treatment. So far, most studies performed to investigate the diagnostic accuracy of DECT were done using a special scanner type equipped with two x-ray tubes (dual-source CT), which is not generally available.

DECT with VNCa could identify BME and thus might replace MRI in certain cases. The aim of our study was to assess the diagnostic accuracy of DECT with VNCa (here performed using a single-source technique [22, 23]) for identification of BME in a larger cohort of patients in comparison to MRI as the standard of reference.

## Methods

### Ethics approval and consent

The study was approved by the local ethics committee (EA1/372/14). Authorisation by the German Federal Office for Radiation Protection (BfS) was waived by the ethics committee and the German Society of Radiology (DRG). All patients gave written informed consent.

### Patients

We prospectively included patients consecutively presenting to our orthopaedic clinic with back pain and radiographically suspected vertebral compression fracture from January 2015 to February 2017, thus suspicion of an acute fracture. All patients were at least 50 years of age. Exclusion criteria were contraindications to MRI, e.g., implanted defibrillators, and patients not able to give informed consent.

### Imaging

All patients underwent a dual-energy computed tomography (DECT) of the thoracic and/or lumbar spine on a 320-row single-source scanner (Canon Aquilion ONE Vision Edition, Canon Medical Systems, Tochigi, Japan). The CT protocol included a scanogram and a DECT with sequential volume acquisition of the high (135) and low (80) kVp datasets. Automatic exposure control was applied for both energy levels using a noise level of 12 to determine image quality. The rotation time was .275 s with a change over time of .5 s in between the acquisitions.

Primary images were computed with 0.5-mm slice thickness using iterative reconstruction (AIDR 3D standard) and a medium soft tissue kernel without beam hardening compensation for DECT and a sharp bone kernel for morphological evaluations. Software for the reduction of stitching artefacts was applied when a fracture was near the stitching area. VNCa datasets were generated in sagittal orientation with 5-mm averaged slice thickness using the CT console (Dual Energy Image View, Version 6; Canon Medical Systems) with a dual-energy gradient of .69 for calcium and object formulas of 0/0 for water and -136/-106 (80 kV/135 kV) for fat.

Morphological images in bone kernel and 135 kVp soft tissue kernel were reformatted with 2-mm slice thickness in sagittal orientation.

MRI was performed on a 1.5-Tesla scanner (MAGNETOM Avanto; Siemens Healthineers or MAGNETOM Symphony Vision; Siemens Healthineers). The imaging protocol included a T1-weighted (repetition time, TR 551 ms, echo time, TE 12 ms, matrix 448 × 336) and a short-tau inversion recovery (STIR) sequence (TR 6150 ms, TE 31 ms, inversion time 150 ms, matrix 320 × 265) with a slice thickness of 3 mm, a slice interval of 3.3 mm and a field of view of 350 × 350 mm in sagittal orientation.

CT and MRI examinations were performed as soon as they were available and suitable for the patient. Therefore, there was no fixed order of the examinations, and DECT was performed before or after MRI.

## Radiation exposure

The dose-length product (DLP) and the CT dose index (CTDIvol) were determined. The estimated effective dose was calculated using a conversion coefficient of .01 $mSv*mGy^{-1}*cm$.

## Target and reference vertebrae

To provide a specific and meaningful analysis that is close to clinical practice, we decided to include only fractured vertebrae into our analysis. The fractured vertebrae were identified in a consensus reading session of the three readers at least 2 weeks before the individual scoring using height loss in the morphological CT images as a criterion and without access to VNCa reconstructions or MRI images. These vertebrae were defined as target vertebrae but were only included in the analysis if they were covered by the MRI scan. For each patient, a reference vertebra was defined as the most caudal vertebra depicted in both, MRI and DECT, without loss of height or former surgery (e.g. kyphoplasty or metal implants). Only target vertebrae were included in the analysis of BME scores. Reference vertebrae were defined for image quality evaluation only.

## Image reading

Three blinded readers with different experience levels (reader 1: a radiologist specialised in musculoskeletal diseases with 8 years of experience; reader 2: a trauma surgeon with 5 years of experience; reader 3: a research student with 1 year of experience) independently assessed the DECT and MR images. The readers used a semiquantitative scoring system including loss of height according to the Genant classification (0–3) [24] and the presence of BME (0–3 - 0: no oedema; 1: < 33%, 2: 33–66%, 3: > 66% of the vertebral volume) [23]. The readers were not aware which vertebrae were defined as target or reference vertebrae. They had access to all images of the respective modality during scoring (e.g. when scoring VNCa images, they could view the CT images reconstructed in bone kernel to look for sclerosis that might imitate BME).

Furthermore, the three readers were asked to separately evaluate image quality of the generic CT images, VNCa reconstructions, T1-weighted MR images and STIR images using a numerical rating scale ranging from 0 to 10.

## Objective imaging parameters

Reader 3 performed region-of-interest (ROI) measurements for calculation of the signal-to-noise ratio (SNR), contrast-to-noise ratio (CNR) and intervertebral ratio (IVR). A polygonal ROI including the bone marrow of the vertebral body with at least 2-mm distance from the cortical bone and excluding the central vein was defined in sagittal slice orientation in MRI (T1 and STIR), CT source images at 135 kVp and VNCa reconstructions. Mean signal intensity (MRI) and attenuation (DECT) with corresponding standard deviations were determined for target and reference vertebrae in both MRI sequences (T1 and STIR) and two CT reconstructions (CT in soft tissue kernel at 135 kVp and VNCa) in the sagittal plane. Furthermore, the air outside the patients' body was measured in a standardised oval ROI with an area of 3 $mm^2$. SNR, CNR and IVR were calculated according to Eqs. 1–3 [23].

$$SNR = \frac{signal}{noise} = \frac{mean_{TV} - mean_{air}}{standard\ deviation_{air}} \quad (1)$$

Calculation of signal-to-noise ratio, where SNR - signal-to-noise ratio; mean = mean attenuation in HU for DECT (135 kVp source images and VNCa) or mean signal intensity for MRI (T1 or STIR); TV = target vertebra; and air = air outside the patient.

$$CNR = \frac{signal_{pathology} - signal_{normal}}{noise} = \frac{mean_{TV} - mean_{RV}}{standard\ deviation_{air}} \quad (2)$$

Calculation of contrast-to-noise ratio, where CNR = contrast-to-noise ratio; mean = mean attenuation in HU for DECT (135 kVp source images and VNCa) or mean signal intensity for MRI (T1 or STIR); TV = target vertebra; RV = reference vertebra; and air = air outside the patient.

$$IVR = \frac{signal_{pathology} - signal_{normal}}{signal_{normal}} = \frac{mean_{TV} - mean_{RV}}{mean_{RV}} \quad (3)$$

Calculation of intervertebral ratio, where IVR = intervertebral ratio; CNR = contrast-to-noise ratio; mean = mean attenuation in HU for DECT (135 kVp source images and VNCa)

or mean signal intensity for MRI (T1 or STIR); TV = target vertebra; and RV = reference vertebra.

The anonymisation of the patients' identifying information, scoring and measurements were performed on a workstation with a high-resolution monitor using OsiriX (Version 6.4; Pixmeo SARL; Bernex, Switzerland).

### Data analysis

A contingency table analysis was performed to calculate sensitivity, specificity and positive and negative predictive value using the combined results of the three readers of MRI STIR as standard of reference. The sensitivity of each modality for the detection of vertebral fracture was calculated using the consensus reading as standard of reference. Wilcoxon's matched-pairs signed-rank test was used to compare CT and MRI. A BME and Genant score of 1 or higher was defined as positive. Fleiss's κ was calculated for inter-reader reliability of BME scoring based on DECT and MRI. SNR and CNR of both MRI sequences (T1 and STIR) and both CT reconstructions (CT and VNCa) were compared using a one-way ANOVA with multiple comparisons and a Bland-Altman plot. Signal intensities and HU as well as IVR values of vertebrae positive and negative for BME (in STIR MRI) were compared applying a Mann-Whitney U-test separately to T1, STIR, CT and VNCa. Spearman's correlation of the IVR of VNCa with T1, STIR and CT was calculated. For statistical analysis, a vertebra was counted as positive if two of three readers agreed on the presence of BME or fracture. Image quality was compared using the mean scores of all three readers. *P*-values were corrected for multiple comparisons using Tukey's test. We aimed for a sample size of 80 patients including drop-outs based on an expected prevalence of oedema in 70% of the patients and an agreement between both modalities of (intraclass kappa) of .95.

## Results

### Patients

Seventy patients (23 men, 47 women) were included in the analysis. The mean age was 70.7 (SD 9.8, range 51–86) years. The median interval between DECT and MRI was 2 days (mean 4.4 (SD 9.0), maximum 22 days). A flowchart of study inclusion is presented in Fig. 1.

### Radiation exposure

The mean DECT scan length was 3.9 (SD 1.7) lumbar and 4.5 (SD 4.0) thoracic vertebrae. The examinations had a DLP of 582.3 (SD 163.9, range 63.9–1,168.9) mGy*cm and a CTDIvol of 16.2 (SD 1.0, range 4.6–42.1) mGy, corresponding to a mean radiation exposure of 5.8 (SD 1.6) mSv and a mean exposure of .69 mSv per vertebra.

### Target vertebrae

A total of 548 vertebrae were depicted by both DECT and MRI. The analysis included a total of 192 target vertebral bodies – 113 lumbar (59%) and 79 thoracic (41%) vertebrae. Thirteen percent (32/192) of the evaluated vertebral bodies were subject to previous surgery (24 kyphoplasties and nine spinal fusions). Sixty-nine percent (132/192) of the target vertebrae were positive for BME on MRI.

### Image reading

CT detected 98% (188/192) of the vertebral bodies with loss of height (combined scores of all three readers compared to the results of the consensus reading), MRI 93% (178/192), $p = .006$. VNCa detected BME in 59% (114/192) of target vertebrae versus 69% (132/192) in MRI, $p = .02$. Based on MRI, 20% (38/192) of the vertebral bodies were assigned an oedema score of 3, 18% (35/192) a score of 2, and 21% (41/192) a score of 1.

The results of contingency table analysis for the detection of BME in all target vertebrae and those with and without prior surgery are presented in Table 1. The resulting overall diagnostic accuracy was .72. Sensitivity of VNCa increased with oedema extent in MRI (.81 for oedema scores of 2 or higher and .89 for a score of 3). By including all depicted vertebrae in the analysis, the specificity increased to .95. Sensitivity per reader ranged from .62 to .8 and specificity from .46 to .71, depending on the reader's experience in VNCa image interpretation (reader 1: SE .8, SP .71; reader 2: SE .68, SP .63; reader: 3 SE .62, SP .46). Fleiss's κ for the detection of BME was .40 for DECT and .58 for MRI. Imaging examples are provided in Fig. 2.

### Subjective image quality analysis

Mean subjective image quality scores were 7.2 (SD 1.4) for CT, 7.6 (SD 1.8) for T1, 6.4 (SD 1.7) for VNCa and 6.3 (SD 1.8) for STIR. Using multiple comparisons, we found no significant difference between CT and T1 ($p = .37$) or VNCa and STIR ($p = .99$). However, there was a significant difference between the morphological images (CT and T1) and the images used for BME evaluation ($p < .0001$).

### Objective image quality parameters

Unsurprisingly, SNR and CNR were significantly better for T1 compared to STIR, CT and VNCa (see Fig. 3). Interestingly, STIR and VNCa showed no significant differences. A detailed comparison using the Bland-Altman method

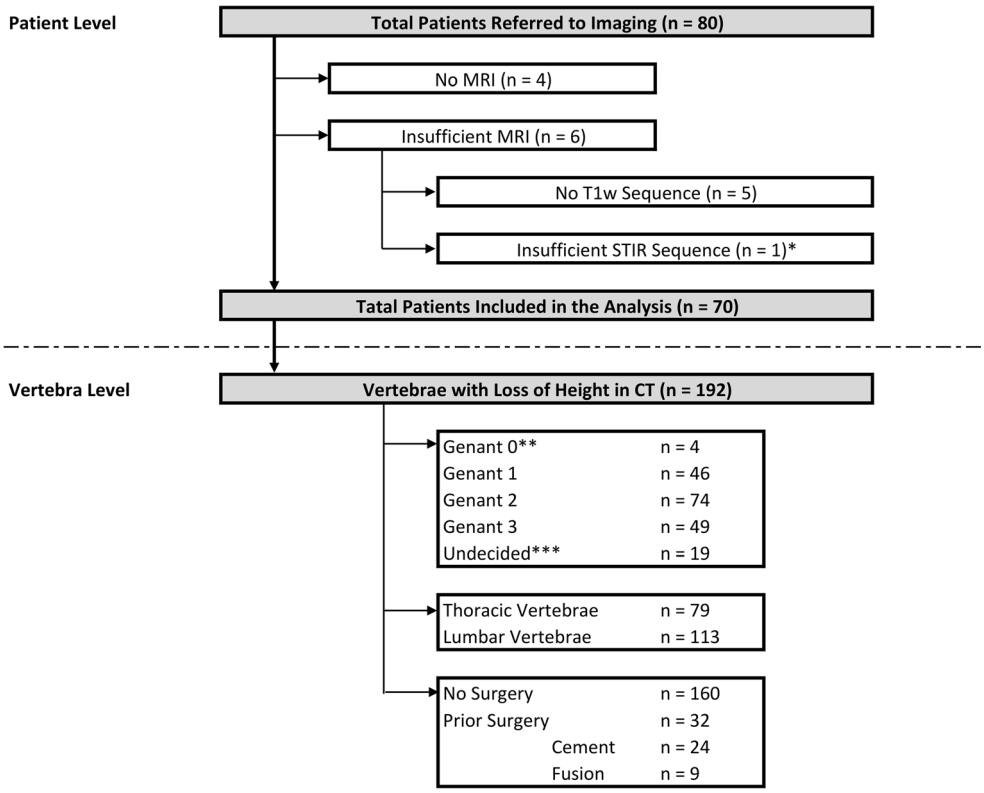


**Fig. 1** Flow chart of study inclusion. On the patient level, all patients who underwent DECT were included (n = 80), while all patients without an MRI examination (n = 4; three of them without evidence of a fracture in CT) or MRI with missing sequences (n = 5) were excluded. *: One patient was excluded from analysis because a coronal rather than a sagittal STIR sequence was obtained (n = 1). On the vertebral level, 192 vertebral bodies with a loss of height identified in a consensus reading were included in the analysis (n = 192). The Genant scores were calculated as the agreement of two of the three readers in DECT independently from the consensus reading. Therefore, four vertebrae were scored as Genant type 0 (**) although they were suspicious in the consensus reading, and in 19 vertebrae each reader assigned a different score (***)

is shown in Fig. S1 (Online Supplementary Material). Vertebral bodies without and with oedema in STIR differed in terms of T1 signal intensities (380.1 (SD 154.9) and 304.1 (SD 141.5), respectively; $p$ of .003). Similar differences were found for STIR (130.2 (SD 57.2) and 175.3 (SD 82.2), $p$ = .0004), CT (85.6 (SD 49.3) and 141.9 (SD 69.6), $p < .0001$), and VNCa images (-32.9 (SD 59.4) and 2.9 (SD 106.2), $p$ = .024). The resulting IVRs are illustrated in Fig. 4. We found a Spearman r of .37 for the correlation of VNCa with T1, .35 for VNCa with STIR and .61 with CT ($p < .0001$ for all correlations).

**Table 1** Contingency table analysis for all target vertebrae (bone marrow oedema, BME) and those with and without prior surgery (w/o surgery and with surgery) based on the combined scorings of the three readers and using MRI as standard of reference

| *BME* | **MRI +** | **MRI -** | **Total** | **SE** | .73 | .64 to .80 |
|---|---|---|---|---|---|---|
| **VNCa +** | 96 | 18 | 114 | **SP** | .7 | .57 to .81 |
| **VNCa -** | 36 | 42 | 78 | **PPV** | .84 | .76 to .90 |
| **Total** | 132 | 60 | 192 | **NPV** | .54 | .42 to .65 |
| *W/o surgery* | **MRI +** | **MRI -** | **total** | **SE** | .79 | .70 to .87 |
| **VNCa +** | 84 | 16 | 100 | **SP** | .7 | .56 to .82 |
| **VNCa -** | 22 | 38 | 60 | **PPV** | .84 | .75 to .91 |
| **Total** | 106 | 54 | 160 | **NPV** | .63 | .50 to .75 |
| *With surgery* | **MRI +** | **MRI -** | **total** | **SE** | .46 | .27 to .67 |
| **VNCa +** | 12 | 2 | 14 | **SP** | .67 | .22 to .96 |
| **VNCa -** | 14 | 4 | 18 | **PPV** | .86 | .57 to .98 |
| **Total** | 26 | 6 | 32 | **NPV** | .22 | .06 to .48 |

The data are given with 95% confidence intervals

Sensitivity for BME increases when excluding vertebrae with prior surgery. This indicates that BME might be obscured by artefacts in those patients, while specificity is not affected All values were calculated based on the agreement of two of the three readers

*SE* sensitivity, *SP* specificity, *PPV* positive predictive value, *NPV* negative predictive value

## Discussion

In our study, we found a reasonably high sensitivity (.73) and specificity (.7 for target vertebrae only and .95 for all vertebrae; see below) of DECT with VNCa for the detection of BME in patients with osteoporosis-associated vertebral compression fractures aged 50 years or older. Sensitivity increases with the amount of oedema identified in MRI (up to .89). However, diagnostic accuracy strongly varied with the readers' experience in VNCa image interpretation. In vertebrae with prior surgery, sensitivity for BME was markedly lower than in those without (.46 vs .79). This also resulted in an inferior inter-rater reliability of VNCa (.32 to .48) versus MRI (.56 to .62). Subjective image quality scores did not differ between VNCa and STIR images ($p > .99$), nor did objective image quality measured by CNR and SNR. However, analysis of signal intensities and IVR revealed differences between fractures with and without oedema for all

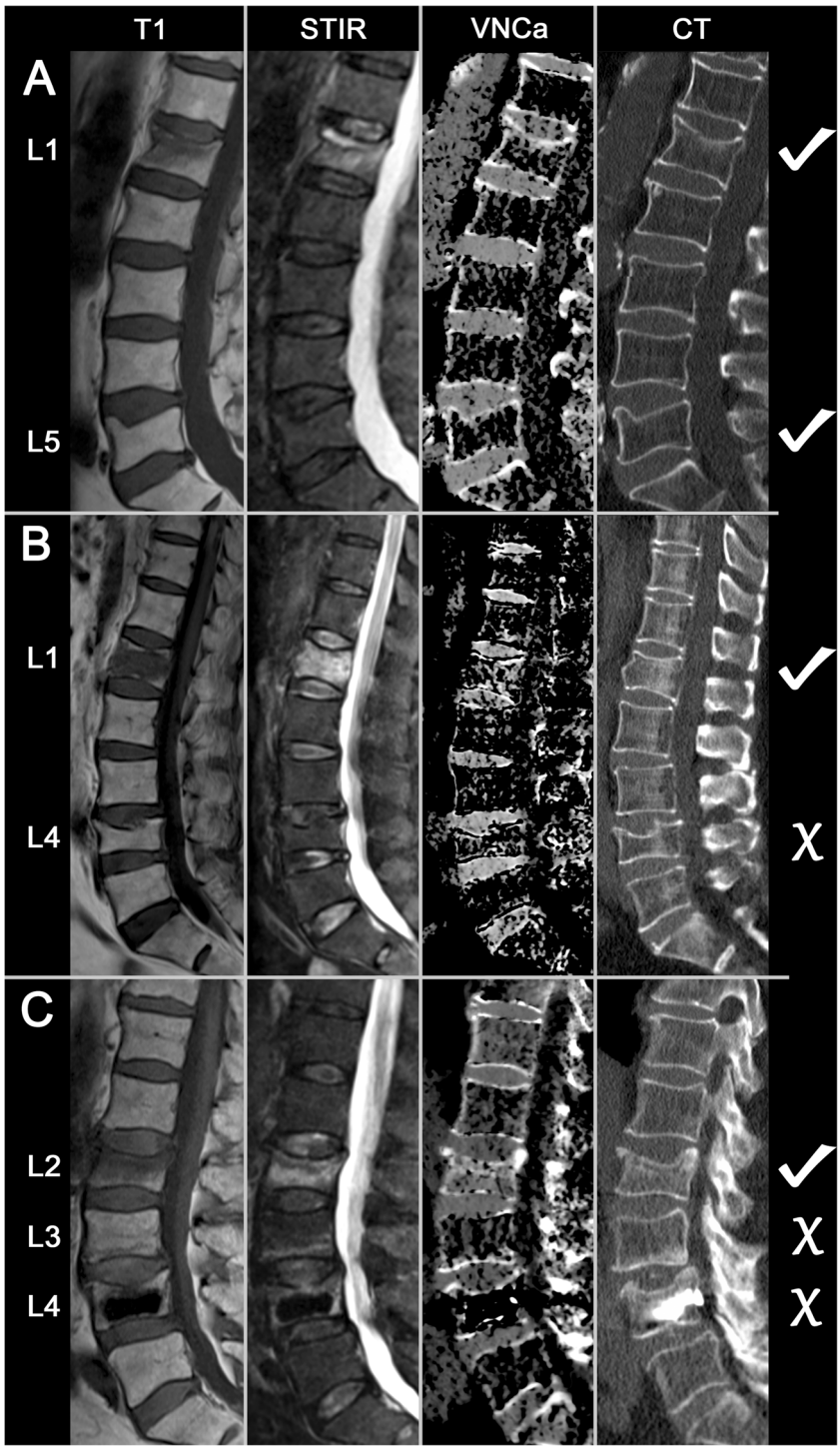


**Fig. 2** Imaging examples from three different patients. For each patient (left to right) T1, STIR, VNCa and bone kernel reconstructions of DECT scans are shown. (A) An 83-year-old male with a fresh compression fracture at L1 showing decreased signal intensity in T1 combined with increased signal in STIR because of BME (3/3 readers). VNCa shows increased density, indicating BME (3/3) – true positive. L5 has a loss of height; however, no signal changes in MRI (0/3) and normal density in VNCa (0/3) – true negative. (B) A 76-year-old female patient with a fresh pathological fracture of L1 in MRI (3/3) and corresponding increase in density in VNCa (3/3) – true positive. However, areas with replacement of normal bone marrow cannot be distinguished from bone marrow oedema using VNCa. L4 shows a loss of height without bone marrow changes in MRI (0/3) but increased density in VNCa (2/3) – false positive. (C) A 73-year-old female showing a fresh fracture of L2 with BME in MRI (3/3) and VNCa (3/3) – true positive. L3 shows an irregularity of the endplate with small band-like BME (3/3) that can easily be missed in VNCa (1/3) – false negative. L4 with prior kyphoplasty with discrete oedema surrounding the cement (3/3); however, no oedema in VNCa (1/3) – false negative

sequences and both modalities, especially when compared to the normal bone marrow (e.g., a reference vertebra).

DECT might be a useful diagnostic tool for the evaluation of BME in older patients with vertebral compression fractures, especially when MRI is not immediately available or in case of contraindications or severe pain. It enables superior characterisation of fracture morphology based on generic CT images combined with assessment of bone marrow using VNCa. DECT may be used to decide if a patient can be discharged home or has to remain in hospital for further diagnostic work-up. Most analyses indicate that DECT can be achieved with similar image quality and radiation exposure when compared to conventional single energy examinations [25, 26]. However, an experienced reader is needed for image interpretation. Therefore, we recommend an additional MRI in suspicious or unclear cases. Further studies are needed to

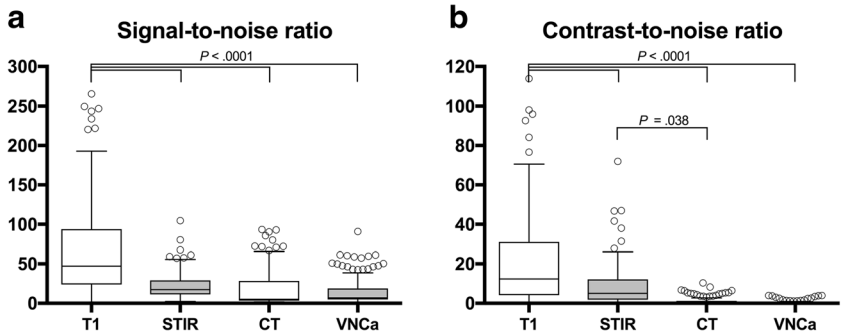


**Fig. 3** Signal- (**a**) and contrast- (**b**) to-noise ratios for T1, STIR, CT and VNCa. SNR and CNR are significantly higher for T1 than the other images. There is also a small significant difference in CNR for STIR and CT. *P*-values were calculated using a one-way ANOVA with multiple comparisons and were corrected using Tukey's test. Some outliers are seen for each modality due to a few examinations with exceptionally low image noise

corroborate our findings and further define which kind of patients can be examined by DECT imaging alone and which patients should undergo an additional MRI.

Furthermore, based on our analysis, MRI may be superior to DECT for assessment of vertebral bodies operated on before – despite previous reports suggesting the opposite [27] that used the same technique. This is because of a high effective atomic number and inclusion of contrast media cement after balloon kyphoplasty is processed by the algorithm and subtracted from the image. However, in those vertebrae only little bone marrow is left, and thus the interpretation of the images is made difficult. Cement and pedicle screws may also influence the images due to beam-hardening artefacts.

Our results are in line with previous studies performed on other CT scanner types. The sensitivity we found here is in the range reported for dual-source systems (.73 compared to .64 to .89) [18–20, 28]. However, specificity was markedly lower in our study (.7 compared to .97 to 1.0), which can be explained by the fact that our analysis only included vertebrae with a height loss, whereas other studies included all depicted vertebrae, thus artificially inflating the numbers of true-negative samples [18–21, 29]. With inclusion of all vertebrae, specificity in our analysis would increase to .95. However, we believe that our results better reflect the true diagnostic accuracy of DECT in clinical practice. Looking at the performance of the three readers, we found a difference between the most experienced reader (sensitivity and specificity of .8 and .72, respectively) and the least experienced reader (.62 and .46). This is in line with the recent results of Kaup et al, who also found a strong dependency of results on readers' experience [29], and it gives further insights into the application of DECT in daily clinical practice. Whereas objective image parameters (IVR) in our study were able to differentiate fresh from old fractures, there is a significant overlap and artefacts might have an influence on the parameters. This corresponds to a meta-analysis that found better diagnostic accuracy in qualitative compared to quantitative assessment [30].

Some limitations have to be discussed. We included only patients over 50 years of age. Therefore, our results cannot be transferred to younger patients, particularly because they are expected to have a different bone marrow composition. The higher amount of haematopoietic bone marrow that is characterised by an increased density in CT decreases contrast between oedema and bone marrow, impeding the visualisation of BME in DECT. We did not explicitly exclude patients with malignancy. However, only one pathological fracture was included in the analysis (see Fig. 2). Therefore, we do not expect our results to be significantly compromised. We performed CT in volume mode and without table movement between acquisition of the high- and low-kVp datasets. While allowing sequential single-source scanning, this approach results in unique artefacts when the two volumes are stitched together. Readers have to be aware of these artefacts when evaluating the images. Nonetheless, the vendor provides a software

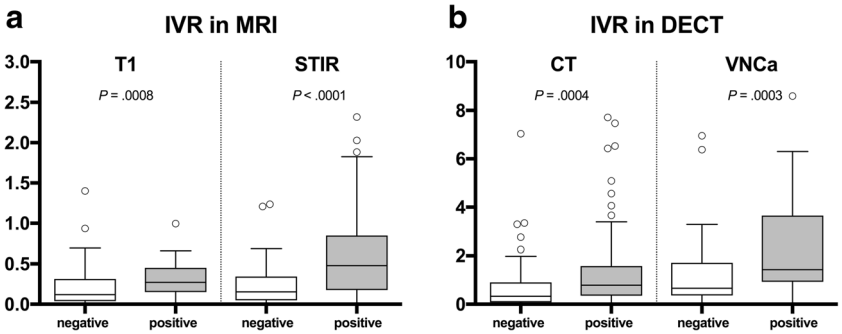


**Fig. 4** Intervertebral ratio (IVR) as defined in Eq. 3 for both MRI sequences (**a**) and DECT (**b**), separately for vertebrae positive and negative for BME in MRI. IVRs are significantly higher in all sequences and reconstructions, indicating good differentiation of vertebrae with (positive) and without (negative) oedema

solution for their reduction. However, compared with fast kVp switching, this technique allows separate adjustment of tube current for each voltage, resulting in lower radiation exposure in the high kVp scan.

Single-source DECT visualises BME with adequate sensitivity and specificity when VNCa reconstructions are used. IVRs measured in VNCa correlate weakly but significantly with those in T1-weighted and STIR images, indicating that VNCa reflects the composition of bone marrow. However, further studies are needed to evaluate which patients can undergo DECT alone and which patients require an additional MRI examination for accurate diagnosis.

**Funding** The Department of Radiology at Charité – Universitätsmedizin Berlin received a research grant by Canon MS. Canon MS provided the software for image-evaluation. The study itself did not received any funding.

## Compliance with ethical standards

**Guarantor** The scientific guarantor of this publication is Torsten Diekhoff.

**Conflict of interest** The authors of this article declare relationships with the following companies: JM is an employee of Canon MS.

**Statistics and biometry** Andrea Stroux kindly provided statistical advice for this manuscript.

**Informed consent** Written informed consent was obtained from all subjects (patients) in this study.

**Ethical approval** Institutional Review Board approval was obtained.

**Methodology**
- prospective
- cross-sectional study/diagnostic study
- performed at one institution

## References

1. Hiligsmann M, Neuprez A, Buckinx F, Locquet M, Reginster JY (2017) A scoping review of the public health impact of vitamin D-fortified dairy products for fracture prevention. Arch Osteoporos 12:57
2. Kyriakos G, Vidal-Casariesgo A, Quiles-Sanchez LV et al (2016) Osteoporosis management in a real clinical setting: heterogeneity in intervention approach and discrepancy in treatment rates when compared with the NOGG and NOF guidelines. Exp Clin Endocrinol Diabetes 124:466–473
3. Cunningham TD, Martin BC, DeShields SC, Romero CC (2016) The impact of osteoporotic fractures compared with other health conditions in older adults living in Virginia, United States. Osteoporos Int 27:2979–2988
4. Cauley JA, Lui LY, Paudel ML et al (2016) Impact of radiographic vertebral fractures on inpatient healthcare utilization in older women. Bone 88:165–169
5. Jackson SA, Tenenhouse A, Robertson L (2000) Vertebral fracture definition from population-based data: preliminary results from the Canadian Multicenter Osteoporosis Study (CaMos). Osteoporos Int 11:680–687
6. Ensrud KE, Thompson DE, Cauley JA et al (2000) Prevalent vertebral deformities predict mortality and hospitalization in older women with low bone mass. Fracture Intervention Trial Research Group. J Am Geriatr Soc 48:241–249
7. Garfin SR, Buckley RA, Ledlie J (2006) Balloon kyphoplasty for symptomatic vertebral body compression fractures results in rapid, significant, and sustained improvements in back pain, function, and quality of life for elderly patients. Spine (Phila Pa 1976) 31:2213–2220
8. Sander AL, Laurer H, Lehnert T et al (2013) A clinically useful classification of traumatic intervertebral disk lesions. AJR Am J Roentgenol 200:618–623
9. Dudli S, Ferguson SJ, Haschtmann D (2014) Severity and pattern of post-traumatic intervertebral disc degeneration depend on the type of injury. Spine J 14:1256–1264
10. Campbell SE, Phillips CD, Dubovsky E, Cail WS, Omary RA (1995) The value of CT in determining potential instability of simple wedge-compression fractures of the lumbar spine. AJNR Am J Neuroradiol 16:1385–1392
11. McConnell CT Jr, Wippold FJ 2nd, Ray CE Jr et al (2014) ACR appropriateness criteria management of vertebral compression fractures. J Am Coll Radiol 11:757–763
12. Wong CC, McGirt MJ (2013) Vertebral compression fractures: a review of current management and multimodal therapy. J multidiscip healthc 6:205–214
13. McCarthy J, Davis A (2016) Diagnosis and Management of Vertebral Compression Fractures. Am Fam Physician 94:44–50
14. Emery DJ, Forster AJ, Shojania KG, Magnan S, Tubman M, Feasby TE (2009) Management of MRI Wait Lists in Canada. Healthc Policy 4:76–86
15. Nicolaou S, Liang T, Murphy DT, Korzan JR, Ouellette H, Munk P (2012) Dual-energy CT: a promising new technique for assessment of the musculoskeletal system. AJR Am J Roentgenol 199:S78–S86
16. De Cecco CN, Schoepf UJ, Steinbach L et al (2017) White paper of the society of computed body tomography and magnetic resonance on dual-energy CT, part 3: vascular, cardiac, pulmonary, and musculoskeletal applications. J Comput Assist Tomogr 41:1–7
17. Reagan AC, Mallinson PI, O'Connell T et al (2014) Dual-energy computed tomographic virtual noncalcium algorithm for detection of bone marrow edema in acute fractures: early experiences. J Comput Assist Tomogr 38:802–805
18. Petritsch B, Kosmala A, Weng AM et al (2017) Vertebral compression fractures: third-generation dual-energy CT for detection of bone marrow edema at visual and quantitative analyses. Radiology 284:161–168
19. Karaca L, Yuceler Z, Kantarci M et al (2016) The feasibility of dual-energy CT in differentiation of vertebral compression fractures. Br J Radiol 89:20150300
20. Bierry G, Venkatasamy A, Kremer S, Dosch JC, Dietemann JL (2014) Dual-energy CT in vertebral compression fractures: performance of visual and quantitative analysis for bone marrow edema demonstration with comparison to MRI. Skeletal Radiol 43:485–492
21. Wang CK, Tsai JM, Chuang MT, Wang MT, Huang KY, Lin RM (2013) Bone marrow edema in vertebral compression fractures: detection with dual-energy CT. Radiology 269:525–533
22. Gondim Teixeira PA, Gervaise A, Louis M et al (2015) Musculoskeletal wide detector CT: principles, techniques and applications in clinical practice and research. Eur J Radiol 84:892–900
23. Diekhoff T, Hermann KG, Pumberger M, Hamm B, Putzier M, Fuchs M (2017) Dual-energy CT virtual non-calcium technique

for detection of bone marrow edema in patients with vertebral fractures: A prospective feasibility study on a single- source volume CT scanner. Eur J Radiol 87:59–65
24. Genant HK, Wu CY, van Kuijk C, Nevitt MC (1993) Vertebral fracture assessment using a semiquantitative technique. J Bone Miner Res 8:1137–1148
25. Foley WD, Shuman WP, Siegel MJ et al (2016) White Paper of the Society of Computed Body Tomography and Magnetic Resonance on Dual-Energy CT, Part 2: Radiation Dose and Iodine Sensitivity. J Comput Assist Tomogr 40:846–850
26. Tao SM, Li X, Schoepf UJ et al (2018) Comparison of the effect of radiation exposure from dual-energy CT versus single-energy CT on double-strand breaks at CT pulmonary angiography. Eur J Radiol 101:92–96
27. Fuchs M, Putzier M, Pumberger M, Hermann KG, Diekhoff T (2016) Acute vertebral fracture after spinal fusion: a case report illustrating the added value of single-source dual-energy computed tomography to magnetic resonance imaging in a patient with spinal Instrumentation. Skeletal Radiol 45:1303–1306
28. Li M, Qu Y, Song B (2017) Meta-analysis of dual-energy computed tomography virtual non-calcium imaging to detect bone marrow edema. Eur J Radiol 95:124–129
29. Kaup M, Wichmann JL, Scholtz JE et al (2016) Dual-energy CT-based display of bone marrow edema in osteoporotic vertebral compression fractures: impact on diagnostic accuracy of radiologists with varying levels of experience in correlation to MR imaging. Radiology 280:510–519
30. Suh CH, Yun SJ, Jin W, Lee SH, Park SY, Ryu CW (2018) Diagnostic performance of dual-energy CT for the detection of bone marrow oedema: a systematic review and meta-analysis. Eur Radiol. https://doi.org/10.1007/s00330-018-5411-5